



Swansea University  
Prifysgol Abertawe



## Cronfa - Swansea University Open Access Repository

---

This is an author produced version of a paper published in :

Cronfa URL for this paper:

<http://cronfa.swan.ac.uk/Record/cronfa8257>

---

### Conference contribution :

Essa, E., Xie, X., Sazonov, I. & Nithiarasu, P. (2011). *Local Phase based Automatic VIUS Media-Adventitia Border Detection.*

[http://dx.doi.org/ na](http://dx.doi.org/na)

---

This article is brought to you by Swansea University. Any person downloading material is agreeing to abide by the terms of the repository licence. Authors are personally responsible for adhering to publisher restrictions or conditions. When uploading content they are required to comply with their publisher agreement and the SHERPA RoMEO database to judge whether or not it is copyright safe to add this version of the paper to this repository.

<http://www.swansea.ac.uk/iss/researchsupport/cronfa-support/>

## LOCAL PHASE BASED AUTOMATIC IVUS MEDIA-ADVENTITIA BORDER DETECTION

Ehab Essa\*, Xianghua Xie\*, Igor Sazonov\*\*, and Perumal Nithiarasu\*\*

\*Department of Computer Science, Swansea University, UK

\*\*College of Engineering, Swansea University, UK

### ABSTRACT

We present a fully automatic segmentation method to extract media-adventitia border in IVUS images. We use a double-interface automatic graph cut technique to prevent the extraction of media-adventitia border from being distracted by those image features. Novel cost functions are derived from using a combination of symmetric and asymmetric local phase features with complementary texture features. Comparative studies on manual labeled data show promising performance of the proposed method.

**Key Words:** *IVUS, media-adventitia border, local phase, optimal interface segmentation.*

## 1 INTRODUCTION

Intra-vascular Ultrasound (IVUS) is a catheter-based technology where an ultrasound probe is moving inside the artery, transmitting signals and receiving the backscattered one from the inside and outside the artery that help to diagnosis of atherosclerosis diseases. Media-adventitia border is the outer side of the artery wall which can be used to measure the circumference, radius and 3D reconstruction of the artery. The appearance and visibility of the media-adventitia border are affected by artery diseases, and acoustic shadow artifacts.

Many techniques have been used in IVUS segmentation such as active contour and level set [1,2] and Graph search [3,4], which one based on minimizing a cost function that is derived from image features and possibly combined with shape prior to refine the segmentation. This approach is also adapted in [5] to deal with 3D volumetric segmentation using s-t cut algorithm to find the minimum closed graph.

Local phase features have shown to be an effective alternative to intensity derived features to deal with inhomogeneity, low image quality, and acoustic shadow that are common in ultrasound images. For example, in [6] it is used to find acoustic boundaries in echocardiography images. Two features can be extracted from local phase analysis: feature symmetry and feature asymmetry. Feature symmetry highlights the location of high congruency between objects in images. Since the media layer has generally uniform characteristics it can be detected by its symmetric feature, whileas feature asymmetry responds to edge-like feature and it can detect potential borders.

This paper presents a fully automated segmentation of media-adventitia border in 2D IVUS images. Double interface segmentation is introduced to obtain the media-adventitia border by combining image driven features with geometric constrains in well defined graph construction to overcome the impediments such as stents, calcification or plaque. The first interface removes any

distraction existed above the media-adventitia border and the second interface finds the border based on the characteristics of media layer.

## 2 PROPOSED METHOD

Briefly, the IVUS images are first transformed from Cartesian coordinates to polar coordinates, height field like, then removing catheter-ring down artifact. Two node-weighted directed graph are then constructed so that the border extraction is considered as computing a minimum closed set graph by using s-t cut algorithm. The extracted media adventitia border from the second graph is smoothed using radial basis function (RBF).

### 2.1 Graph construction

In [7], the authors proposed a novel graph construction method, which transforms the surface segmentation in 3D into computing a minimum closed set in a directed graph. We adapt this method to a 2D segmentation, which can carry out double-interface segmentation simultaneously in low order polynomial time complexity and does not require user initialization. For each desired interface, construct a graph  $G = \langle V, E \rangle$ , where each node  $V(x, y)$  corresponds to a pixel in 2D image  $I(x, y)$ . Along each column in graph, each node is connected to the precedence node in the same column, and then connected to other node in different column to construct the closed graph. After constructing the graph for each of the two interfaces, taking into account interrelations between them is necessary and this is achieved by setting up another set of arcs to connect them. Geometrical constraints can be imposed by setting minimum  $\delta_{min}$  and maximum  $\delta_{max}$  separation distances. The two interfaces thus will not intersect or overlap.

### 2.2 Feature extraction

Local phase features – Two types of features can be extracted from phase congruency: feature asymmetry  $FA(x, y)$  and feature symmetry  $FS(x, y)$ . Feature asymmetry highlights step-like image patterns, and is defined as [6]:

$$FA(x, y) = \sum_m \frac{[|o_m(x, y)| - |e_m(x, y)|] - T_m}{A_m(x, y) + \varepsilon} \quad (1)$$

where  $m$  denotes filter orientation,  $o_m(x, y)$  and  $e_m(x, y)$  are odd and even symmetric Log Gabor filter,  $\varepsilon$  is a small constant,  $T_m$  is an orientation-dependent noise threshold,  $A_m(x, y) = \sqrt{e_m^2(x, y) + o_m^2(x, y)}$  and  $[\cdot]$  denotes zeroing negative values. Feature symmetry favors bar-like image patterns, which is useful in extracting the thin media layer. We modify the feature symmetry equation in [6] to focus only on the dark polarity (minimum intensity) symmetry by:

$$FS(x, y) = \sum_m \frac{[-|e_m(x, y)| - |o_m(x, y)|] - T_m}{A_m(x, y) + \varepsilon} \quad (2)$$

First order derivative of Gaussian – This set of filters is designed to highlight the intensity difference between media and adventitia. Four different orientations are used.

Band-pass log-Gabor – Log Gabor is used as a bandpass filter in three scales to enhance the border and to reduce speckles and other image artifacts. This process is carried out in coarser scales, i.e. in the 3rd, 4th and 5th scales. Hence, these features particularly show dominant edges.

## 2.3 Cost function

For the media-adventitia border, all the three types of features described in Sect. 2.3 are used. It takes the following form:

$$C_1(x, y) = C_d(x, y) + \alpha_1 G(x, y) + \alpha_2(1 - FS(x, y)) \quad (3)$$

where  $C_d$  denotes the term for derivative of Gaussian features,  $C_G$  is for log-Gabor, and  $\alpha_1$  and  $\alpha_2$  are constants.  $C_G$  can be obtained by cascading the filtering responses across scales. However, more weight can be assigned to coarser scale features so that it presence the connectivity of media-adventitia border at the existence of acoustic shadow, e.g.  $C_G = G^{(3)} + G^{(4)} + 1.5G^{(5)}$  as used here and  $G^{(i)}$  denotes *ith* scale. Feature symmetry  $FS$  is useful in enhancing the thin layer of media. It is normalized beforehand, and since the middle of the layer has larger values  $1-FS$  is used in the cost function so that the interface between media and adventitia is highlighted. Note that each of the term in the cost function is normalized. For the auxiliary interface that is above media-adventitia, we use a combination of log- Gabor feature and feature asymmetry:

$$C_2(x, y) = C_G(x, y) + \alpha_3(1 - FA(x, y)) \quad (4)$$

where  $\alpha_3$  is a constant. The combination of those two types of features leads the cost function to favor linking globally dominant image features, which very often is distractive for media-adventitia border segmentation.

## 2.4 Compute the minimum closed set

Each graph node is weighted by a value represents its rank to be selected in the minimum closed set graph where the arc costs between graph nodes are infinitive. The weight assignment is carried out according to  $w(x, y) = C(x, y) - C(x, y - 1)$  where  $C$  denotes the cost function and  $w$  is the weight for each node in the directed graph, which serves as the base for dividing the nodes into non-negative and negative sets. The  $s - t$  cut method can then be used to find the minimum closed set. The source  $s$  is connected to each negative node and every non-negative node is connected to the sink  $t$ , both through a directed arc that carries the absolute value of the cost node itself.

## 2.5 Post-processing

The segmented media-adventitia may still contain local oscillations. Smoothing based post-processing can be adopted to eliminate such oscillations. Here, RBF interpolation using thin plate base function is used to effectively obtain the final interface.

# 3 EXPERIMENTAL RESULTS

A total of 95 IVUS images from 4 acquisitions of 2 patients are used to evaluate the proposed method. These images contain various forms of soft and fibrous plaque, calcification, stent, and acoustic shadow. In most of the images, For all the tested images, ground-truth via manual labeling is available for quantitative analysis. All the parameters are fixed: distance between two surfaces are set as  $\delta_{min} = 5$ ,  $\delta_{max} = 140$ , and cost function weightings are set as  $\alpha_1 = 0.7$ ,  $\alpha_2 = 0.5$ , and  $\alpha_3 = 0.5$ .

The proposed method was compared against the single-interface segmentation with the cost function in (3). The cost function for the media-adventitia was kept the same. Fig. 1 The single-interface segmentation gave partial media-adventitia border, as shown in first row (b). However,

Table 1: comparison between single-interface and double-interface segmentation results. AD: area difference in percentage; AMD: absolute mean difference in pixel compared to ground-truth.

	Single interface		Double-interface AD AMD	
	AD	AMD	AD	AMD
Mean	9.99	12.55	5.84	6.99
Std.	11.06	11.45	4.53	4.13
Min	1.60	1.76	1.47	1.75
Max	57.08	54.70	25.04	24.42

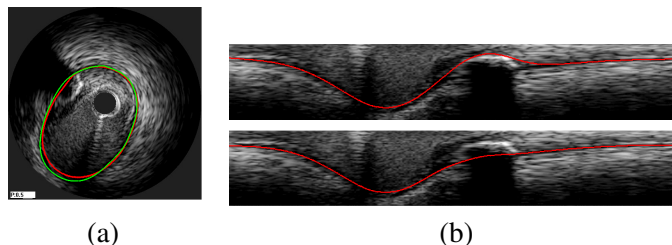


Figure 1: (a) Comparison between ground-truth (green) and the proposed method (red), (b) first row shows single-interface result, and second row shows the proposed method.

its performance degraded when there were interfering image structures. Table 1 provides the quantitative comparison between single-interface approach and the proposed method. The proposed method achieved better accuracy and consistency.

## 4 CONCLUSION

We presented an automatic double-interface segmentation method, whose cost functions combine local and global image features and its geometric constrain is integrated in graph construction. Qualitative and quantitative comparison showed superior performance of the proposed method.

## REFERENCES

- [1] E. Brusseau et al., "Fully automatic luminal contour segmentation in intracoronary ultrasound imaging-a statistical approach," *IEEE Trans Med Imaging*, vol. 23 No. 5, pp. 554-66, 2004.
- [2] M. Plissiti et al., "An Automated Method for Lumen and Media-Adventitia Border Detection in a Sequence of IVUS Frames," *IEEE Trans Inf Technol Biomed*, Vol. 8, No. 2, pp. 131-141, 2004.
- [3] M. Sonka et al., "Segmentation of intravascular ultrasound images: A knowledge-based approach," *T-MI*, vol. 14, No. 4, pp. 719-732, 1995.
- [4] A. Takagi et al., "Automated contour detection for high frequency intravascular ultrasound imaging: A technique with blood noise reduction for edge enhancement," *Ultrasound Med. Biol.*, vol. 26, pp. 1033-1041, 2000.
- [5] A. Wahle et al., "Plaque development, vessel curvature, and wall shear stress in coronary arteries assessed by X-ray angiography and intravascular ultrasound," *Medical image analysis*, vol. 10, no. 4, pp. 615-31, 2006.
- [6] M.Mulet-Parada and J.Noble, "2D + T acoustic boundary detection in echocardiography," *Medical Image Analysis*, vol. 4, no. 1, pp. 21-30, 2000.
- [7] K.Li, et al., "Optimal surface segmentation in volumetric images-a graph-theoretic approach," *T-PAMI*, vol. 28, no. 1, pp. 119-34, 2006.